

Mono- and Binuclear Zinc Complexes with a Bidentate Phenol-Containing 2-Benzylideneamino-5-Methylphenol Schiff Base

N. A. Protasenko^a, S. V. Baryshnikova^a, T. V. Astaf'eva^a, A. V. Cherkasov^a, and A. I. Poddel'sky^a, *

^a Razuvayev Institute of Organometallic Chemistry, Russian Academy of Sciences, Nizhny Novgorod, Russia

*e-mail: aip@iomc.ras.ru

Received December 29, 2020; revised January 4, 2021; accepted January 11, 2021

Abstract—The reaction of zinc chloride with 2-benzylideneamino-5-methylphenol (LH), a bidentate Schiff base, in 1 : 1 molar ratio in the presence of triethylamine gives the ionic complex $[\text{Et}_3\text{NH}]^+[\text{LZnCl}_2]^-$ (**I**). The reaction between the zinc salt (chloride or acetate) and LH in 1 : 2 ratio results in complete displacement of the zinc salt anions to give bis-*o*-iminophenolate ZnL_2 (**II**), which exists in the crystalline state as the $(\text{ZnL}_2)_2$ dimer formed via μ -bridging oxygen atoms of two out of the four *o*-iminophenolate ligands. The molecular structure of ligand LH and complexes **I** and $(\text{II}\cdot\text{CDCl}_3)_2$ was established by X-ray diffraction (CIF files CCDC nos. 2052647 (LH), 2052645 (**I**), 2052646 (**II** \cdot CDCl_3)₂).

Keywords: Schiff base, *o*-iminophenol, zinc, mononuclear, binuclear complex, X-ray diffraction

DOI: 10.1134/S1070328421060038

INTRODUCTION

Schiff bases are widely used as ligands in coordination chemistry [1–3], and complexes based on them are applied in various areas of science and technology: in catalysis, organic synthesis, and analytical chemistry [4–7]; in biochemistry and medicine as components of antibacterial, antifungal, and anticancer drugs [8–13], as luminescent materials, optical and electrochemical sensors [14–17], etc. Schiff bases derived from phenol have been most studied in coordination chemistry. For *o*-iminophenols, complexes with the vast majority of metals are known. However, it is noteworthy that metal complexes with tri-, tetra-, and polydentate Schiff bases and with functional derivatives containing additional coordinating groups are most widely presented in the literature. Data on the complexes with bidentate *o*-iminophenolates are less abundant: for example, the search through the CCDC of 2020 for main group metal complexes of *o*-iminophenolates based on only tridentate 2-benzylideneamino-phenol with an additional coordinating group in position 2 of the benzene ring retrieves 220 structures, while for bidentate 2-benzylideneaminophenol derivatives, only 10 examples are found. There are only two known structurally characterized zinc complexes with bidentate *o*-iminophenolates [18, 19]. However, generally, this class of main group metal complexes is undoubtedly of interest not only for applied studies of light-emitting properties or biochemical activity, but also for fundamental studies of molecular and electronic structures. In this study, we synthesized a simple bidentate ligand, 2-benzylideneamino-5-methyl-

phenol, and performed its reactions with zinc chloride and acetate.

EXPERIMENTAL

The synthesis, isolation, and study of properties of the complexes were carried out in evacuated tubes in the absence of oxygen. Organic solvents were purified by standard procedures [20].

Synthesis of 2-benzylideneamino-5-methylphenol (LH). Benzaldehyde (0.82 mL, 8 mmol) was added dropwise at room temperature to a solution of 2-amino-5-methylphenol (1000 mg, 8 mmol) in methanol (100 mL). The reaction mixture was refluxed with continuous stirring for 8 h and then left overnight at -18°C . The finely crystalline yellow precipitate of LH was separated by filtration, washed with cold methanol, and dried. The yield of LH was 1.35 g (80%).

For $\text{C}_{14}\text{H}_{13}\text{NO}$

Anal. calcd., %	C, 79.59	H, 6.20	N, 6.63
Found, %	C, 79.65	H, 6.24	N, 6.47

IR (Nujol; ν , cm^{-1}): 3397 s, 3059 w, 3034 w, 2953 w, 2924 s, 2855 s, 2729 w, 1892 w, 1874 w, 1628 s, 1579 s, 1531 w, 1499 s, 1332 s, 1295 m, 1260 m, 1243 w, 1221 m, 1184 m, 1170 w, 1156 s, 1123 w, 1100 w, 1072 m, 1025 w, 1007 m, 967 s, 944 s, 870 s, 801 s, 763 s, 692 s, 628 w, 619 w, 584 s, 512 s, 480 m.

¹H NMR (CDCl₃; 400 MHz; δ, ppm): 2.35 (s, 3H, CH₃), 6.72 (d, *J* = 8.1 Hz, 1H, arom. C₆H₃), 6.85 (s, 1H, arom. C₆H₃), 7.22 (d, *J* = 8.1 Hz, 1H, arom. C₆H₃), 7.44–7.51 (m, 3H, arom. C₆H₅), 7.87–7.94 (m, 2H, arom. C₆H₅), 8.68 (s, 1H, –HC=N–). ¹³C NMR (CDCl₃; 100 MHz; δ, ppm): 21.49, 115.45, 115.59, 120.88, 128.68, 128.65, 131.45, 132.87, 136.02, 139.48, 152.30, 155.74.

The crystals of LH suitable for X-ray diffraction were obtained by recrystallization from methanol after the ligand solution was kept at –18°C for 24 h.

Synthesis of [Et₃NH]⁺[LZnCl₂][–] (I). A solution of LH (101 mg, 0.48 mmol) in THF was added to a solution of zinc chloride (65 mg, 0.48 mmol) in THF. After the addition of a stoichiometric amount of Et₃N, the solution color turned orange. The reaction mixture was stirred for 5 h and then the solvent was completely removed. The solid residue was recrystallized from CH₂Cl₂ at room temperature. Complex I was obtained as small cubic yellow crystals suitable for X-ray diffraction. The yield of I was 150 mg (70%).

For C₂₀H₂₈N₂OCl₂Zn

Anal. calcd., % C, 53.53 H, 6.29 N, 6.24 Cl, 15.80
Found, % C, 53.67 H, 6.37 N, 6.09 Cl, 15.69

IR (Nujol; ν, cm^{–1}): 2630 m, 2430 m, 1615 s, 1597 m, 1592 m, 1576 m, 1485 s, 1391 s, 1304 s, 1265 s, 1171 s, 1123 w, 1069 w, 1044 w, 1018 m, 957 s, 893 m, 858 w, 839 m, 800 s, 756 s, 735 s, 677 s, 646 w, 621 w, 605 s, 578 s, 517 w, 488 w.

¹H NMR (CDCl₃; 400 MHz; δ, ppm): 1.31 (t, *J* = 7.3 Hz, 9H, CH₃, Et₃NH⁺), 2.25 (s, 3H, CH₃), 3.26 (q, *J* = 7.3 Hz, 6H, CH₂, Et₃NH⁺), 6.42 (s, 1H, arom. C₆H₃), 6.47 (d, *J* = 8.1 Hz, 1H, arom. C₆H₃), 7.23 (t, *J* = 8.1 Hz, 1H, arom. C₆H₃), 7.44–7.60 (m, 3H, arom. C₆H₅), 8.14 (s, 2H, arom. C₆H₅), 8.76 (s, 1H, CH=N), 10.7 (br.s, 1H, NH). ¹³C NMR (CDCl₃; 100 MHz; δ, ppm): 8.68, 21.54, 45.81, 116.76, 117.47, 118.95, 129.05, 130.11, 132.80, 132.87, 133.18, 140.92, 158.46.

Synthesis of ZnL₂ (II). A solution of LH (287 mg, 1.36 mmol) in methanol (30 mL) was added to a solution of zinc acetate (150 mg, 0.68 mmol) in methanol (20 mL). The resulting solution was heated for 30 min at ~50°C, which resulted in a yellow-orange precipitate of II·CH₃OH. The yield of II·CH₃OH was 275 mg (78%).

For C₂₈H₂₄N₂O₂Zn·CH₃OH

Anal. calcd., % C, 67.25 H, 5.45 N, 5.41
Found, % C, 67.26 H, 5.48 N, 5.22

IR (Nujol; ν, cm^{–1}): 3246 w, 1611 s, 1590 s, 1572 s, 1484 s, 1420 m, 1302 s, 1275 s, 1260 s, 1238 w, 1165 s,

1123 m, 1078 w, 1042 m, 1001 w, 951 s, 891 m, 856 m, 793 s, 758 s, 740 s, 690 s, 648 w, 603 s, 586 m, 520 m, 488 w.

¹H NMR (CDCl₃; 400 MHz; δ, ppm): 2.33 (s, 6H, CH₃), 3.49 (s, 3H, MeOH), 6.39 (d, *J* = 7.9 Hz, 2H, arom. C₆H₃), 6.85 (s, 2H, arom. C₆H₃), 9.95–7.55 (m, 12H, arom. C₆H₅ + C₆H₃), 8.17 (s, 2H, CH=N). ¹H NMR (pyridine-d₅; 400 MHz; δ, ppm): 2.26 (s, 6H, CH₃), 6.48 (d, *J* = 8.1 Hz, 2H, arom. C₆H₃), 7.11–7.23 (m, 10H, arom. C₆H₅), 8.23 (d, *J* = 7.3 Hz, 4H, arom. C₆H₃), 8.68 (s, 2H, CH=N). ¹³C NMR (pyridine-d₅; 100 MHz; δ, ppm): 21.45, 115.73, 117.87, 121.75, 128.86, 130.40, 131.31, 136.56, 140.63, 157.33, 165.10.

Recrystallization of II·CH₃OH from chloroform at a temperature of 0°C gives a sample of complex II without solvating solvent molecules, readily soluble in pyridine. The crystals of complex (II·CDCl₃)₂, suitable for X-ray diffraction, were formed from a dilute solution in CDCl₃ by slow evaporation at room temperature.

¹H and ¹³C NMR spectra were recorded on a Bruker Avance HD-400 spectrometer (operating at 400 MHz; with tetramethylsilane as the internal standard; CDCl₃ and pyridine-d₅ as solvents), IR spectra were measured on an FSN-1201 FTIR spectrometer (400–4000 cm^{–1} range; Nujol). Elemental analysis was carried out by pyrolytic method with a gravimetric finish.

X-ray diffraction study of LH, I, and (II·CDCl₃)₂ was carried out on Bruker D8 Quest (LH, *T* = 100 K) and Rigaku OD Xcalibur (I, (II·CDCl₃)₂, *T* = 293 K) diffractometers (MoK_α radiation, ω scan mode, $\lambda = 0.71073 \text{ \AA}$). The experimental sets of intensities were collected and integrated using APEX3 [21] and CrysAlisPro [22] program packages. The absorption corrections were applied and the structures were solved and refined using ABSPack (CrysAlisPro), SADABS [23], and SHELX [24] program packages. The structures were solved by direct methods and refined by full-matrix least squares on F_{hkl}^2 in the anisotropic approximation for non-hydrogen atoms. The hydroxyl hydrogen atom of LH and the ammonium hydrogen atom of I were found from the difference Fourier maps. All other hydrogen atoms of LH, I, and (II·CDCl₃)₂ were placed into geometrically calculated positions and refined isotropically with fixed thermal parameters $U(H)_{\text{iso}} = 1.2U(C)_{\text{equiv}}$ ($U(H)_{\text{iso}} = 1.5U(C)_{\text{equiv}}$ for methyl groups). Crystallographic data and X-ray diffraction experiment and structure refinement details for LH, I, and (II·CDCl₃)₂ are summarized in Table 1. The structures are deposited with the Cambridge Crystallographic Data Centre (CCDC nos. 2052647 (LH), 2052645 (I), 2052646 (II·CDCl₃)₂; deposit@ccdc.cam.ac.uk or <http://www.ccdc.cam.ac.uk>).

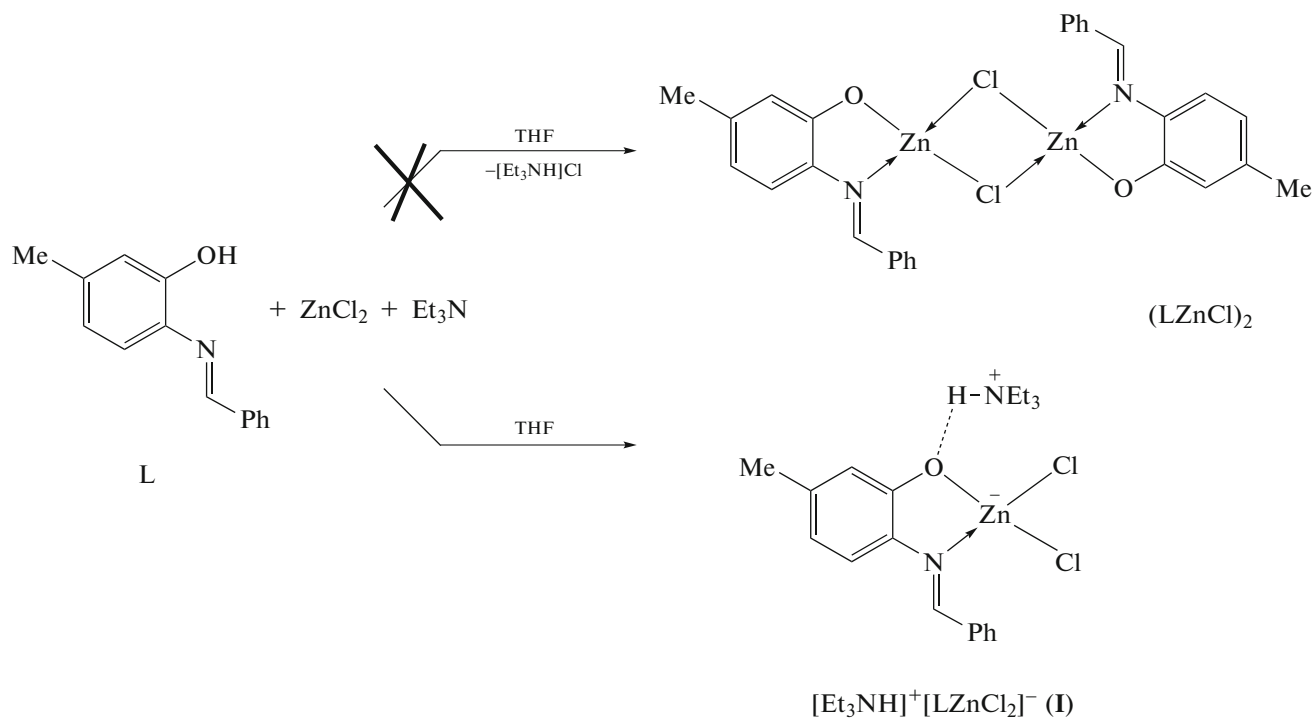
Table 1. Crystallographic data and X-ray experiment and structure refinement details for compounds LH, **I**, and **(II·CDCl₃)₂**

Parameter	Value		
	LH	I	(II·CDCl₃)₂
Molecular formula	C ₁₄ H ₁₃ NO	C ₂₀ H ₂₈ N ₂ OCl ₂ Zn	C ₅₆ H ₄₈ N ₄ O ₄ Zn ₂ ·2CDCl ₃
<i>M</i>	211.25	448.71	1212.47
System	Orthorhombic	Orthorhombic	Triclinic
Space group	<i>P</i> 2 ₁ 2 ₁ 2 ₁	<i>P</i> na2 ₁	<i>P</i> 1̄
<i>a</i> , Å	5.8851(5)	9.2463(3)	10.4125(2)
<i>b</i> , Å	7.8119(6)	23.8870(9)	11.4282(2)
<i>c</i> , Å	23.674(2)	10.0411(4)	12.1855(2)
α, deg	90	90	103.436(2)
β, deg	90	90	93.747(2)
γ, deg	90	90	95.509(2)
<i>V</i> , Å ³	1088.37(15)	2217.74(14)	1398.06(4)
<i>Z</i>	4	4	1
<i>F</i> (000)	448	936	620
ρ(calcd.), g/cm ³	1.289	1.344	1.440
μ, mm ⁻¹	0.081	1.359	1.194
Crystal size, mm	0.40 × 0.17 × 0.15	0.41 × 0.31 × 0.16	0.27 × 0.22 × 0.11
Range of θ, deg	2.75–27.14	3.12–28.68	2.92–28.70
Ranges of reflection indices	−7 ≤ <i>h</i> ≤ 7, −10 ≤ <i>k</i> ≤ 10, −30 ≤ <i>l</i> ≤ 30	−12 ≤ <i>h</i> ≤ 12, −32 ≤ <i>k</i> ≤ 32, −13 ≤ <i>l</i> ≤ 13	−14 ≤ <i>h</i> ≤ 14, −15 ≤ <i>k</i> ≤ 15, −16 ≤ <i>l</i> ≤ 16
Number of measured reflections	12755	33359	25342
Number of unique reflections (<i>I</i> > 2σ(<i>I</i>))	2042	4876	5312
<i>R</i> _{int}	0.0392	0.0250	0.0377
<i>S</i> (<i>F</i> ²)	1.048	1.026	1.020
<i>R</i> ₁ /w <i>R</i> ₂ (<i>I</i> > 2σ(<i>I</i>))	0.0504/0.1173	0.0341/0.0866	0.0391/0.0931
<i>R</i> ₁ /w <i>R</i> ₂ (for all data)	0.0610/0.1243	0.0430/0.0913	0.0620/0.1030
Residual electron density (max/min), e/Å ³	0.25/−0.31	0.30/−0.23	0.45/−0.30

RESULTS AND DISCUSSION

The reaction of zinc dichloride with *o*-iminophenol (LH) in the presence of triethylamine can give different products depending on the conditions. In the case of equimolar ratio between *o*-iminophenol LH and the inorganic zinc salt (Scheme 1), the mononuclear ionic complex [Et₃NH]⁺[LZnCl₂][−] (**I**) was iso-

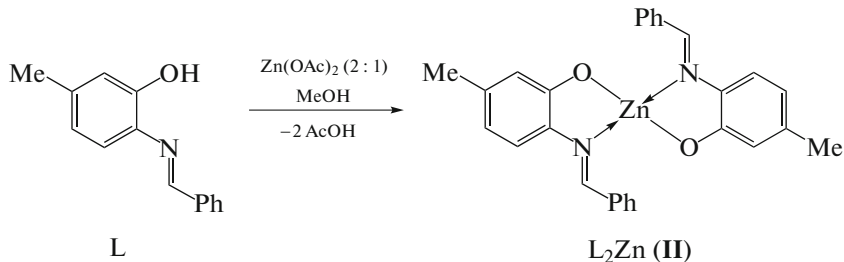
lated, rather than the monoligand neutral complex LZnCl, which should probably exist as chlorine-bridged dimer (LZnCl)₂ (e.g., as in the chloro zinc complexes of the same type with *N,N'*-chelating iminoacenaphthylamide or acenaphthenediimine ligand [25, 26]). Complex **I** was isolated in a pure state and characterized by IR and NMR spectroscopy and X-ray diffraction.



Scheme 1.

The reaction of zinc chloride or acetate with the Schiff base **LH** in 1 : 2 molar ratio in the presence (for zinc chloride) or in the absence of triethylamine (for zinc acetate) is accompanied by complete replacement of the zinc salt anions to give zinc bis-*o*-imino-phenolate ZnL_2 (**II**) (Scheme 2). Fast precipitation from a solution in methanol gives solvate $\text{II} \cdot \text{CH}_3\text{OH}$; however, recrystallization from chloroform gives complex **II** with solvating molecules of the solvent. It

should be noted that complex **II** isolated in this way proved to be poorly soluble in common low-polarity organic solvents. For example, for ^{13}C NMR study, a solution of complex **II** in pyridine- d_5 was prepared. Slow crystallization from a solution of **II** in CDCl_3 for 2 weeks at room temperature resulted in the formation of crystals of complex $(\text{II} \cdot \text{CDCl}_3)_2$, suitable for X-ray diffraction.



Scheme 2.

The molecular structure of complexes **I** and $(\text{II} \cdot \text{CDCl}_3)_2$ in the crystalline state was determined by X-ray diffraction (Figs. 1 and 2, respectively).

The zinc cation in **I** is bound to two chloro ligands and to the nitrogen and oxygen atoms of the *o*-imino-phenolate ligand. Thus, the metal coordination number is 4, and its coordination environment is a distorted tetrahedron (Fig. 1). The dihedral angle between the ClZnCl and OZnN planes is $85.41(8)^\circ$.

The $\text{Zn}-\text{Cl}$ bond lengths are in the $2.219(2)$ – $2.230(2)$ Å range. The $\text{Zn}(1)-\text{O}(1)$ distance ($1.970(3)$ Å) is somewhat shorter than the sum of the covalent radii of these atoms ($\text{Zn } 1.34$, $\text{O } 0.73$ Å) [27]. The $\text{Zn}(1)-\text{N}(1)$ distance ($2.081(3)$ Å) is comparable with the sum of the covalent radii ($\text{Zn } 1.34$, $\text{N } 0.74$ Å) [27], although this is a donor–acceptor bond. The C–C bond distribution in the C(1–6) six-membered ring of the *o*-imino-phenolate ligand ($1.384(6)$ – $1.401(4)$ Å) definitely points to the aromatic nature of this moiety. The

O(1)–C(1) and N(1)–C(1) single bond lengths in **I** are 1.336(4) and 1.432(4) Å, respectively; they are somewhat shorter than these bonds in the initial LH (1.363(3), 1.417(3) Å) and are comparable with the O–C (1.32–1.36 Å) and N–C (1.38–1.43 Å) distances in other transition metal [28–32] and main group metal [33–37] (imino)phenolate complexes.

Thus, LZnCl_2^- is an anion. The Et_3NH^+ cation coordinated to oxygen of the *o*-iminophenolate ligand serves as the counterion in **I**.

Compound $(\text{II}\cdot\text{CDCl}_3)_2$ is the dimeric zinc(II) complex in which the Zn^{2+} cation is bound to two oxygen atoms and two nitrogen atoms of two *o*-iminophenolate ligands. One of the oxygen atoms (O(2)) is additionally coordinated to the second metal atom and thus occupies a bridging position. Thus, the coordination number of zinc(II) cations is 5, and the coordination environment is a distorted trigonal bipyramidal, the base of which is formed by the O(1), O(2), and N(1) atoms, and the vertices are occupied by N(2) and O(2') (for the Zn(1) atom) (Fig. 2).

The Zn(1)–O(1) and Zn(1)–O(2) bond lengths in $(\text{II}\cdot\text{CDCl}_3)_2$ differ little (1.941(2), 1.935(2) Å, respectively) and are comparable with the Zn–O distance in **I** (1.970(3) Å). The Zn(1)–O(2') distance is 2.197(2) Å and exceeds the sum of the covalent radii of the elements [27]. The Zn–N distances in the terminal and bridging ligands are nonequivalent. The Zn(1)–N(1) bond length (2.068(2) Å) is even somewhat shorter than that in **I** (2.081(3) Å), whereas the Zn(1)–N(2) distance (2.363(2) Å) is substantially greater than the sum of the covalent radii of the corresponding atoms [27]. The O–C and N–C bond lengths are in the 1.330(2)–1.345(2) and 1.418(2)–1.1423(2) Å ranges, respectively. Note that the O(1)–C(1) distance (1.330(2) Å) in the terminal *o*-iminophenolate ligand of $(\text{II}\cdot\text{CDCl}_3)_2$ is somewhat shorter than the O(2)–C(15) bond length (1.345(2) Å) in the bridging *o*-iminophenolate. Changes of this type, in some cases more pronounced, take place upon the formation of bridging μ -oxo bonds in catecholate, *o*-amidophenolate, and related metal complexes [37–42]. As in **I**, C–C bond length distribution in the C(1–6) and C(15–20) six-membered rings of the *o*-iminophenolate ligands (1.373(3)–1.419(3) Å) attests to the aromatic nature of these moieties.

The O(1)…C(1S) distances between oxygen of the terminal *o*-iminophenolate ligand and the carbon atom of the CDCl_3 solvation molecule are in the 2.99(2)–3.15(2) Å range and are indicative of intermolecular interactions in $(\text{II}\cdot\text{CDCl}_3)_2$. Thus, the dimer $(\text{II}\cdot\text{CDCl}_3)_2$ with additionally coordinated chloroform molecules can be represented as shown in Scheme 3.

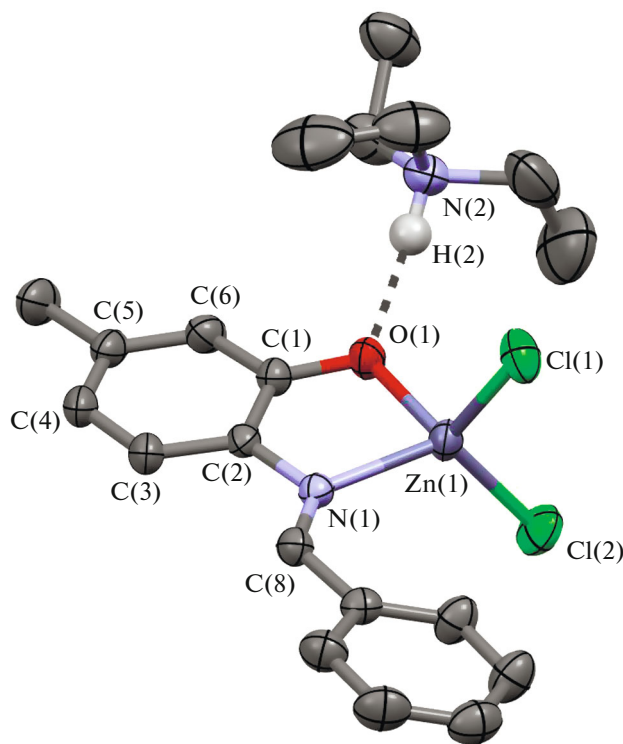
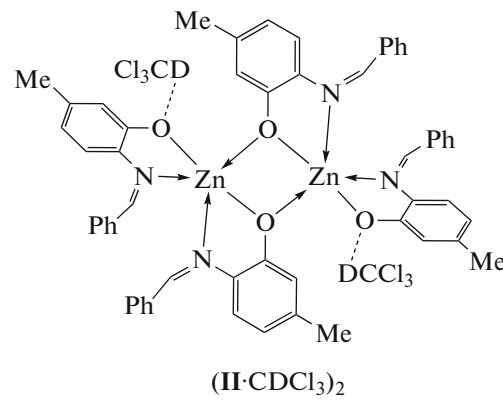


Fig. 1. Molecular structure of **I**. Hydrogen atoms, except for the Et_3NH^+ group proton, are omitted for clarity. Thermal ellipsoids are drawn at the 50% probability level. Selected bond lengths: Zn(1)–O(1), 1.970(3); Zn(1)–N(1), 2.081(3); Zn(1)–Cl(1), 2.230(2); Zn(1)–Cl(2), 2.219(2); O(1)–C(1), 1.335(4); N(1)–C(2), 1.433(4); N(1)–C(8), 1.276(5); C(1)–C(2), 1.400(5); C(1)–C(6), 1.399(5); C(2)–C(3), 1.402(4); C(3)–C(4), 1.384(5); C(4)–C(5), 1.370(6); C(5)–C(6), 1.386(6); N(2)–H(2), 1.12(5) Å.



Scheme 3.

Thus, we studied the reaction of zinc salts with 2-benzylideneamino-5-methylphenol. When zinc chloride and this *o*-iminophenol were taken in an equimolar ratio and reacted in the presence of triethylamine, the reaction gave an ionic compound containing dichloro zinc *o*-iminophenolate anion and triethylammonium cation. When the zinc salt and *o*-imino-

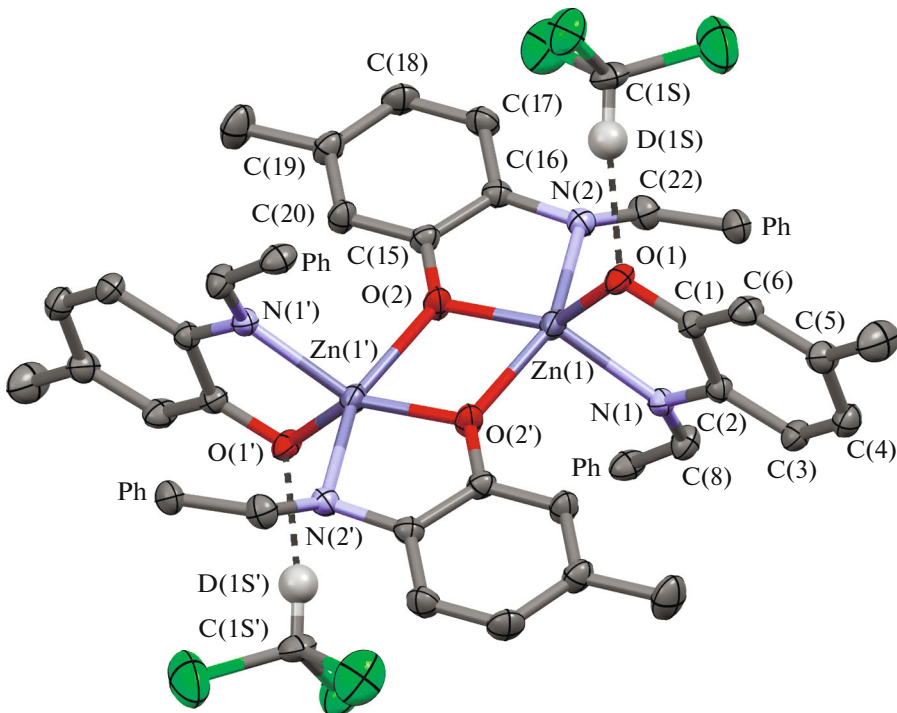


Fig. 2. Molecular structure of $(\text{II}\cdot\text{CDCl}_3)_2$. Hydrogen atoms and phenyl CH groups are omitted for clarity. Thermal ellipsoids are drawn at the 50% probability level. Selected bond lengths: $\text{Zn}(1)-\text{O}(1)$, 1.941(2); $\text{Zn}(1)-\text{O}(2)$, 1.935(2); $\text{Zn}(1)-\text{O}(2')$, 2.197(2); $\text{Zn}(1)-\text{N}(1)$, 2.068(2); $\text{Zn}(1)-\text{N}(2)$, 2.363(2); $\text{O}(1)-\text{C}(1)$, 1.330(2); $\text{O}(2)-\text{C}(15)$, 1.345(2); $\text{N}(1)-\text{C}(2)$, 1.423(2); $\text{N}(1)-\text{C}(8)$, 1.279(2); $\text{N}(2)-\text{C}(16)$, 1.418(2); $\text{N}(2)-\text{C}(22)$, 1.285(3); $\text{C}(1)-\text{C}(2)$, 1.419(3); $\text{C}(1)-\text{C}(6)$, 1.397(3); $\text{C}(2)-\text{C}(3)$, 1.395(3); $\text{C}(3)-\text{C}(4)$, 1.379(3); $\text{C}(4)-\text{C}(5)$, 1.393(3); $\text{C}(5)-\text{C}(6)$, 1.388(3); $\text{C}(15)-\text{C}(16)$, 1.402(3); $\text{C}(15)-\text{C}(20)$, 1.387(3); $\text{C}(16)-\text{C}(17)$, 1.393(3); $\text{C}(17)-\text{C}(18)$, 1.373(3); $\text{C}(18)-\text{C}(19)$, 1.391(3); $\text{C}(19)-\text{C}(20)$, 1.388(3) Å.

phenol molar ratio was 1 : 2, the reaction gave zinc bis-*o*-iminophenolate, existing in the crystal as a dimer. The dimer is formed due to the bridging positions of the oxygen atoms of two out of the four *o*-iminophenolate ligands.

ACKNOWLEDGMENTS

The studies were performed using research equipment of the Center for Collective Use “Analytical Center of the Razuvaev Institute of Organometallic Chemistry, Russian Academy of Sciences” at the Razuvaev Institute of Organometallic Chemistry, Russian Academy of Sciences.

FUNDING

The studies of zinc salt reactions with *o*-iminophenol were supported by the Russian Foundation for Basic Research (project no. 19-03-00208a); spectroscopic studies were carried out within the framework of state assignment for the Razuvaev Institute of Organometallic Chemistry, Russian Academy of Sciences.

CONFLICT OF INTEREST

The authors declare that they have no conflicts of interest.

REFERENCES

1. Vigato, P.A. and Tamburini, S., *Coord. Chem. Rev.*, 2004, vol. 248, nos. 17–20, p. 1717.
2. Liu, X. and Hamon, J.-R., *Coord. Chem. Rev.*, 2019, vol. 389, p. 94.
3. Miroslaw, B., *Int. J. Mol. Sci.*, 2020, vol. 21, no. 10, p. 3493.
4. Clarke, R.M. and Storr, T., *Dalton Trans.*, 2014, vol. 43, no. 25, p. 9380.
5. Liu, X., Manzur, C., Novoa, N., et al., *Coord. Chem. Rev.*, 2018, vol. 357, p. 144.
6. Zoubi, W.A., Al-Hamdani, A.A.S., and Kaseem, M., *Appl. Organomet. Chem.*, 2016, vol. 30, no. 10, p. 810.
7. Gupta, K.C. and Sutar, A.K., *Coord. Chem. Rev.*, 2008, vol. 252, nos. 12–14, p. 1420.
8. Hameed, A., Rashida, M., Uroos, M., et al., *Exp. Opin. Ther. Pat.*, 2017, vol. 27, no. 1, p. 63.
9. Hossain, M.S., Roy, P.K., Zakaria, C.M., et al., *Int. J. Chem. Stud.*, 2018, vol. 6, no. 1, p. 19.
10. Kumar, M., Abbas, Z., Tuli, H.S., and Rani, A., *Curr. Pharmacol. Rep.*, 2020, vol. 6, p. 167.
11. Kaczmarek, M.T., Zabiszak, M., Nowak, M., and Jas-trzab, R., *Coord. Chem. Rev.*, 2018, vol. 370, p. 42.
12. More, M.S., Joshi, P.G., Mishra, Y.K., and Khanna, P.K., *Mater. Today Chem.*, 2019, vol. 14, p. 100195.

13. Malik, M.A., Dar, O.A., Gull, P., et al., *Med. Chem. Commun.*, 2018, vol. 9, no. 3, p. 409.
14. Berhanu, A.L., Gaurav, I., Mohiuddin, A.K., et al., *Trends Anal. Chem.*, 2019, vol. 116, p. 74.
15. Zhang, J., Xu, L., and Wong, W.-Y., *Coord. Chem. Rev.*, 2018, vol. 355, p. 180.
16. Oiye, É.N., Ribeiro, M.F.M., Katayama, J.M.T., et al., *CRC Crit. Rev. Anal. Chem.*, 2019, vol. 49, no. 6, p. 488.
17. Udhayakumari, D. and Inbaraj, V., *J. Fluoresc.*, 2020, vol. 30, p. 1203.
18. Garnovsky, A.D., Antsyshkina, A.S., Sadikov, G.G., et al., *Russ. J. Inorg. Chem.*, 1995, vol. 40, p. 64.
19. Kim, Y.-I., Yun, S.-J., Hwang, I.-H., et al., *Acta Crystallogr., Sect. E: Struct. Rep. Online*, 2012, vol. 68, p. m504.
20. Gordon, A. and Ford, R., *The Chemist's Companion: A Handbook of Practical Data, Techniques, and References*, New York: Wiley, 1972.
21. *Bruker APEX3*, Madison: Bruker AXS Inc., 2015.
22. *Rigaku Oxford Diffraction. CrysAlisPro. Version 1.171.38.46*, Wroclaw: Rigaku Corporation, 2015.
23. Krause, L., Herbst-Irmer, R., Sheldrick, G.M., and Stalke, D., *J. Appl. Crystallogr.*, 2015, vol. 48, no. 1, p. 3.
24. Sheldrick, G.M., *Acta Crystallogr., Sect. C: Struct. Chem.*, 2015, vol. 71, no. 1, p. 3.
25. Fedushkin, I.L., Tishkina, A.N., Fukin, G.K., et al., *Eur. J. Inorg. Chem.*, 2008, no. 3, p. 483.
26. Fedushkin, I.L., Skatova, A.A., Ketkov, S.Y., et al., *Angew. Chem., Int. Ed. Engl.*, 2007, vol. 46, p. 4302.
27. Batsanov, S.S. *Russ. J. Inorg. Chem.*, 1991, vol. 36, p. 1694.
28. Briel, O., Fehn, A., Polborn, K., and Beck, W., *Polyhedron*, 1999, vol. 18, nos. 1–2, p. 225.
29. Novoa, N., Roisnel, T., and Hamon, P., *Dalton Trans.*, 2015, vol. 44, no. 41, p. 18019.
30. Perez, S., Lopez, C., Caubet, A., et al., *J. Organomet. Chem.*, 2007, vol. 692, p. 2402.
31. Pérez, S., López, C., Caubet, A., et al., *Eur. J. Inorg. Chem.*, 2008, vol. 2008, p. 1599.
32. Baryshnikova, S.V., Poddel'sky, A.I., Cherkasov, A.V., and Smolyaninov, I.V., *Inorg. Chim. Acta*, 2019, vol. 495, p. 118963.
33. Baryshnikova, S.V., Bellan, E.V., Poddel'sky, A.I., et al., *Inorg. Chem. Commun.*, 2016, vol. 69, p. 94.
34. Baryshnikova, S.V., Bellan, E.V., Poddel'sky, A.I., et al., *Eur. J. Inorg. Chem.*, 2016, vol. 2016, no. 33, p. 5230.
35. Poddel'sky, A.I., Arsenyev, M.V., Astaf'eva, T.V., et al., *J. Organomet. Chem.*, 2017, vol. 835, p. 17.
36. Poddel'sky, A.I., Astaf'eva, T.V., et al., *J. Organomet. Chem.*, 2018, vol. 873, p. 57.
37. Baryshnikova, S.V., Poddel'sky, A.I., Bellan, E.V., et al., *Inorg. Chem.*, 2020, vol. 59, no. 10, p. 6774.
38. Elmali, A., Elerman, Y., Zeyrek, C.T., and Svoboda, I., *Z. Naturforsch. B: J. Chem. Sci.*, 2003, vol. 58, no. 5, p. 433.
39. Wong, J.L., Sanchez, R.H., Logan, J.G., et al., *Chem. Sci.*, 2013, vol. 4, no. 4, p. 1906.
40. Klementyeva, S.V., Smolentsev, A.I., Abramov, P.A., and Konchenko, S.N., *Inorg. Chem. Commun.*, 2017, vol. 86, p. 154.
41. Klementyeva, S.V., Lukyanov, A.N., Afonin, M.Yu., et al., *Dalton Trans.*, 2019, vol. 48, p. 3338.
42. Piskunov, A.V., Maleeva, A.V., Meshcheryakova, I.N., and Fukin, G.K., *Russ. J. Coord. Chem.*, 2013, vol. 39, p. 245.
<https://doi.org/10.1134/S107032841303007X>
43. Meshcheryakova, I.N., Shavyrin, A.S., Cherkasov, A.V., and Piskunov, A.V., *Izv. Akad. Nauk, Ser. Khim.*, 2019, no. 7, p. 1414.

Translated by Z. Svitanko